3D printing of mortar with continuous fibres: principle, properties and potential for application

Jean-François Caron, Léo Demont, Nicolas Ducoulombier, Romain Mesnil

3D printing of mortar with continuous fibers: principle, properties and potential for application

Jean-François Caron[a,*], Nicolas Ducoulombier[a], Léo Demont[a], Romain Mesnil[b]

[a] *Navier Laboratory, École des Ponts ParisTech, Univ. Gustave Eiffel, CNRS, Marne-La-Vallée, France*

[b] *École des Ponts ParisTech, Marne-La-Vallée, France*

Abstract

Important developments in additive manufacturing with concrete have been achieved in the past decades. Yet, printed components usually do not comply with building standards or basic reliability principles, and are not commonly used as load-bearing components. A gap between research and practice exists and despite several attempts, off-the-shelf commercial solutions for the reinforcement of the 3D printed structural components seem always expected. This article presents a patented alternative for reinforcement of 3D printed structures. This technology inspired by the composite industry is called *flow-based pultrusion for additive manufacturing*. A strict control of the rheological behaviour of the cementitious matrix ensures the routing and impregnation of continuous yarns of thin fibres (glass, basalt, etc.). The resulting material, *Anisotropic Concrete* homogeneously reinforced in a single direction, provides enhanced strength and ductility. This paper describes the process, its constraints, and first experimental achievements. It also lists and proposes new applications of the technology beyond conventional applications of concrete printing. New possibilities about the process itself and extrusion strategies, but also new imaginable constructive solutions and structural applications. Some of them are inspired by composite material industry.

Keywords: additive manufacturing, pultrusion, concrete printing, composite materials, fibre reinforced concrete, anisotropic concrete

*Corresponding author
E-mail: jean-francois.caron@enpc.fr

1. Introduction

The cement industry contributes about 5% to global anthropogenic CO2 emissions. In [1], authors estimated in a very complete study, that total carbon emissions from cement production in 1994 were 307 million metric tons of carbon (MtC), 160 MtC from process carbon emissions, and 147 MtC from energy use. In 2016, the estimation reached 1450 MtC [2]! It's considerable and this drastic increase these last decades, due in part to the more recent Chinese consumption, challenges to reduce the amount of cement. Of course, using other materials, as steel or wood may help to this aim. But the optimisation of concrete structure designs and implementing *the right material at the right place* is also necessary. Digital technologies, like large-scale 3d printing are a step in this direction because they allow for more complex structures, which have a chance to be more sustainable. However, reinforcement of such structures is still a vastly open question.

Several reinforcement strategies have been proposed during the last century to improve the tensile strength and ductility of concrete. Metallic rebars are undoubtedly the most conventional reinforcement: they are cheap, optimised, and easy to install. Rebars can carry the tensile forces thanks to a good anchorage in the concrete. They distribute stresses in the concrete favouring micro-cracks at the expense of disastrous macro cracks. Fibre-Reinforced Plastic rebars exist since the 1980's [3, 4] but remain anecdotal and devoted to very specific situations, due to a higher cost and lower stiffness. For example, their durability is an asset when rapid internal corrosion of steel rebars is a problem [5].

But glass, carbon, basalt fibres may also be used directly (without polymer impregnation) as constituents of technical fabrics used in replacement of more rigid rebars [6]. They are easier to handle and to shape (complex geometries), but also less efficient structurally as classical pouring techniques make it difficult to obtain a good impregnation of yarns (gathering thousand of microfibres) and a good shear transfer in concrete. Short fibres mixed in the fresh concrete before pouring, like in Ultra-High-performance Fibre Reinforced Concretes (UHP

FRC), are nowadays a classical and efficient solution and provide post-cracking behaviour. However, due to the necessary workability of the fresh mix, the fibre ratios remain low, and 2 or 3% represent a hard job to achieve. Many studies concern these topics (see for example [7]).

The pre-tensioning or post-tensioning of rebars or cables is also a technical solution that decreases the tensile stresses in the concrete, increasing thus the load-bearing capacity of the structure. Pre-stress is mainly used to connect prefabricated components of large structures like bridges. These components can be manufactured with 3D printing, as proposed in [8] or [9]. However, pre-stressing technology deals more at the structural scale than at the material scale, which is the focus of this article.

More specifically the purpose of this paper is to propose a solution to reinforce printed concrete itself. Some strategies already exist in this direction as well and have been reviewed in detail in [10]. Most of those are revisiting classical reinforcement strategies mentioned earlier, using rebars or grids in combination with printed concrete. They are generally developed for non-standard concrete structures and as part of an integrated digital process based on sophisticated robotic fabrication strategies. *Smart Dynamic Casting* and *mesh mould* developed at ETH Zurich [11] propose a robotic concept which allows for the continuous production of a three dimensional welded reinforcement mesh used here as a formwork, and the concrete infill. The technology is based on this porous cage ability to evacuate water excess. At the time of pouring, water contained in the concrete is instantly evacuated through the filtering faces, attenuating thus the hydrostatic pressure. Such sacrificial filtering formworks were first proposed for conventional concrete in France (*Dipy* 1992, $3DR^{®}$ 1999 [12]) and later in China [13]. They permit complex shapes and an attenuation of hydrostatic pressure by more than 80%. The *NEST* building at *Empa* in Zurich implements some experimentations using new 3D printed concrete technologies for freeform columns and roofs, produced without formwork.

Some other proposals address the reinforcement of the extruded lace itself. Interesting experimentation based on an idea firstly presented in [14] consists of

the driving of a reinforcement cable into the extruded concrete lace during printing [15]. Concrete beams have been printed and reinforced with such cables, and the results are encouraging, although the bond between the concrete and the steel cables needs to be improved to avoid the premature slippage observed by authors.

Finally, the addition of short fibres in concrete is also widely investigated since it is an obvious solution. Like for FRC, fibres improve the cracking behaviour even if an increase of the flexural tensile strength is highlighted in the literature. Fibres are mixed before pumping and are thus homogeneously dispersed in the section. Their maximum ratio is limited to a few percent due to pumpability requirements [16] [17]. Interestingly, the authors show that printing significantly aligns the fibres in the flow direction. This leads to a homogeneous anisotropic behaviour of the reinforced lace, which could radically change the design of concrete structures, and lead to breakthrough innovations.

Our proposal, first introduced in [18], fits in this context, allowing much higher fibre ratios and thus even greater anisotropy, due to the alignment of long fibres. We called the process *flow-based pultrusion* and it is now a patented process for extrusion-based additive manufacturing of continuously reinforced mortars. An experimental devoted device including mortar extrusion and fiber's bobins management is now developped. An intimate mix of fibres and matrix ensures the stresses transfer inside the resulting material, which can consequently be considered homogeneous, in the spirit of composite materials. The mixture modelling rules may apply, the framework of continuous mechanics becoming relevant for the estimation of homogeneous mechanical properties.

The process is detailed in the next part, and the potential for this technology will then be discussed.

2. Anisotropic concrete and flow based pultrusion

Adapted to a fully digital environment, the process includes the specific device for mortar extruding, for routing and management of fibers (prototype), a 6

degrees of freedom robotic arm (ABB), and a code permitting the global workflow (based on *HAL Robotics* software). The set permits to build a structure layer by layer through a continuous deposition of material, following a classical robotic path, but the fibering may also proposes more innovative investigations as demonstrated in the second part of the paper. In this process, concrete rather refers to fine cementitious material, such as mortar or paste with a maximal particle size limited to few millimeters, to a good impregnation of the yarns. These continuous multi-fiber yarns are the reinforcement unit and made of mineral or organic fibres, such as Basalt fiber, AR glass fiber or carbon fiber. Monofilaments as 0,1mm steel wires were tried [19] but didn't demonstrate good results due in particular to a too smooth and regular fiber surface, leading to a poor interface quality with mortar. During the process, tens of these continuous yarns are continuously added to the cementitious mortar and pulled by the flow before final deposition. The obtained reinforcement ratio of the *anisotropic concrete*, finally depends on the area proportion of reinforcement in the transversal section of the lace. The first experiments are with only several percent, but a more industrial prototype will permit more than 10

2.1. Extrusion Lace Shaping versus Oriented Lace Pressing

A key point concerning robotic extrusion of concrete, from a material point of view, and without considering fibering, is the mastering of yield stress at nozzle exit and its evolution through time. This viscoplastic material has also a thixotropic behavior and many parameters must be controlled to allow the deposition and the increasing weight of additional laces without buckling collapses. Different printing technologies are classically used, and they belong to 2 main families, Extrusion Lace Shaping (ELS), and Oriented Lace Pressing (OLP).

ELS concerns firm material, with an initial yield stress well above thousands of pascal. During the extrusion, the filament section is prescribed by the nozzle shape. As a consequence, the section of the lace is not changed during deposition. Moreover, the large yield stress value ensures a strong consistency and an

easy deposition of the first couple of layers. This refers to the simplest printing technology, very efficient and reliable. But once the mix is realised, it exists no way to modify the extruded material, neither to adapt at external modifications, nor to propose more sophisticated strategies. For instance, to permit a good impregnation of yarns, it is natural to think about a fluid composition, which has to harden very quickly to avoid the collapse of the stacking of printed laces. This shows all the interest of the other available technology, OLP. OLP is devoted to material with smaller consistency, i.e. for yield stress value around hundreds of Pascals. In this case, the thickness of the layer is prescribed by the distance between the nozzle and the previous layer and its width is given by the conservation of mass. If the width of the extruded lace is superior to the exit diameter of the nozzle, the plastic flow during deposition can induce a pressure peak, proportional to yield stress at the nozzle exit, which needs to be limited to prevent object failure. This regime is often found for high structuration rate material that is achievable using a more sophisticated printing technologies. Indeed, the high structuration rate is provided by the addition of an accelerator additive or viscosity modifier additive (VMA) to the extruded material. A comparison of the evolution of the yield stress during the printing for ELS and OLP is illustrated in Figure 1. An example of such printing device is described in detail in [20]. Thanks to this mastering of the time-dependent rheology of the mortar, OLP is consequently of great interest as may combine first a good impregnation of yarns and then a good mechanical behavior of the stacking of printed laces. OLP is consequently the technology used in our development.

2.2. Flow-based pultrusion versus motorized devices

The proposed *flow-based pultrusion technology* is then very similar to other OLP robotic extrusion technology. The only change is the addition of yarns in the concrete flow just before the nozzle exit. To ensure the driving of the yarns several strategies are possible concerning the application of the mechanical force needed on the yarn. This mechanical work may be brought by rollers,

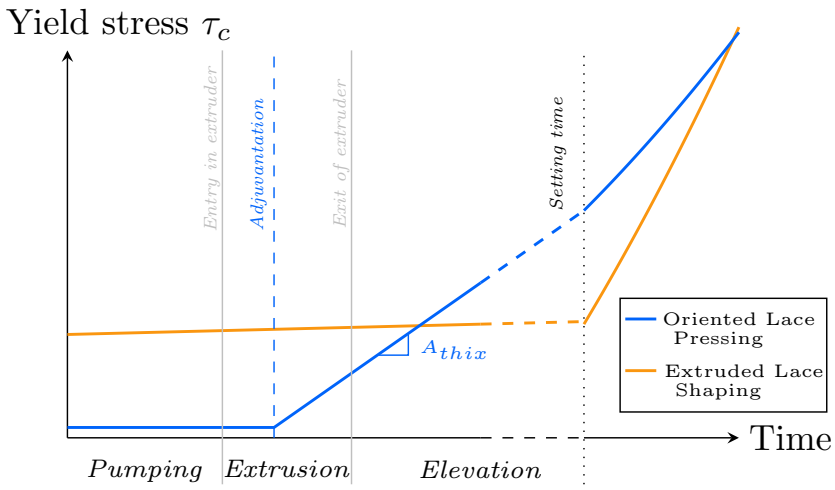

Figure 1: Structuration rate for both asymptotic regime, Extrusion Lace Shaping (ELS) and Oriented Lace Pressing (OLP).

like in bi-extrusion and pultrusion, as defined in Figure 2. In our present solution, the flow-based pultrusion, the mechanical work is provided directly by the shear interaction between the concrete flow and the yarns. The geometry of this nozzle and the adjustable rheological conditions have to ensure enough pulling force on the yarns to drive the reinforcement. A longitudinal principle cut of this nozzle is also illustrated in Figure 2. The evolution of the uniaxial forces applied on the reinforcements during deposition, are also plotted for each process. It is really important to notice that internal force is only in tension for traditional and flow-based pultrusion. On the contrary, pushing force is applied in the co-extrusion process which leads to compressive internal force. This compressive force could limit the minimal radius of the continuous reinforcement unit to avoid buckling issues. However, it would also come with a restriction on the curvature of the printing path, due to the higher flexural rigidity of a larger yarn. On the other hand, reinforcement yarns with smaller diameters increase the specific surface area of reinforcement and consequently the interaction with concrete. This aspect is further discussed in the next paragraph. Another point

is that during a curved path, the inside bend yarn, must have a smaller deposition speed than the outside bend filament. As a consequence, co-extrusion of more than one yarn becomes very difficult for a curved printing path, since reinforcement deposition is made by controlling the speed. This is not the case with flow-based pultrusion, where the deposition of the yarn is controlled by a shear force. The modification of the concrete flows inside the nozzle is expected to play the role of a differential gear.

The yield stress mastering appears definitely as the key point of the technol-

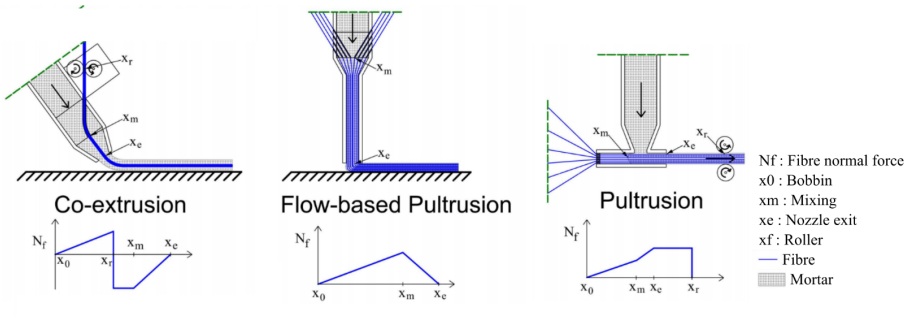

Figure 2: Schema of different continuous reinforcement processes (from [18])

ogy. Numerous conditions exist on the rheology of the concrete during robotic extrusion. They mainly refer to three macroscopic properties of the mortar, well studied in the scientific literature, pumpability, extrudability, and buildability. Here it is important also to be able to estimate the ability to generate a given pulling force on the continuous reinforcement yarn. To do so, a simple analysis is proposed using the hypothesis that maximal interfacial shear stress between yarn and mortar is equal to the yield stress $\tau_c(x)$ of the mortar. Under this condition, the maximal pulling force applied on each yarn with no relative displacement between fibre and mortar, noted F_{max} is given by the integration of the equilibrium of an element of the yarn and is equal to:

$$F_{max} = \int_{x_m}^{x_e} \tau_c(x)\, P \, \mathrm{d}x \tag{1}$$

with P the cumulated perimeter of each fibers of the yarn, x_e: the location

of nozzle exit and x_m the location of mixing, defined in Figure 2. For a constant yield stress, between mixing and nozzle exit, it gives:

$$F_{max} = \tau_c \, P \, l \tag{2}$$

with $l = x_e - x_m$ the yarn-carrying length. But such a mortar is not the better choice to allow a good impregnation, since the yield stress is constant and must be high to permit the driving of the yarn. Mortars with a high structuration rate, permitting a fast increase of the yield stress are more promising. This structuration can be supposed linear with time, as proposed in [21], and another expression for F_{max} using eq.1 can be found. The yield stress before starting the process and at the nozzle exit have to be measured.

On our actual device, the order of magnitude of the necessary force to apply on a yarn to fight against various frictions due to the wire conveyor is 0.1 Newton. The global perimeter of the reinforcement yarn is about 1 mm and the length of the carrying zone is 100 mm. Under that condition, the mean value of the yield stress in the carrying zone should be around 1000 Pa, which is the typical order of magnitude of the yield stress in robotic extrusion. However it is also too high to expect a good impregnation of the yarn, and this confirms the interest of the OLP process (more fluid, hundreds of Pa) including adapted accelerator and length l.

2.3. Why fibre diameter matters

The approach proposed in this article is inspired by composite materials, and as such, a diameter of 0.1mm is considered in the presented experiments. This is a significant difference compared to previous processes implemented in long-fibre extrusion, which used co-extrusion of mortar and rope, with a diameter in the centimetric range [15]. The fibre diameter can indeed be correlated to the quality of the bonding between the fibres and the matrix.

To illustrate this correlation, we consider n fibres of diameter ϕ in a lace of length L and diameter D with a constant volumic fraction η. Such laces are shown in Figure 3. The pull-out force of fibres is closely related to its specific

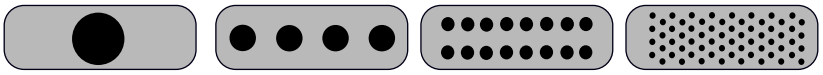

Figure 3: Cross section of laces with the same fibre volume, but different fibre diameter d. The surface area of contact S increases as the diameter decreases.

surface area, i.e. the surface area of contact S between the fibres and the matrix, especially if the latter is homogeneous. First, we consider a constant volumic fraction η of fibres in the lace: writing correspondence between volumes and simplifications leads to equation (3).

$$\eta D^2 = n\phi^2 \tag{3}$$

The surface area of contact between the fibres and the matrix can thus be determined with equation (4).

$$S = n\pi dL = \frac{\eta\pi D^2 L}{\phi} \tag{4}$$

Therefore, the difference between a typical rebar where $\phi \sim 1$cm and the approach proposed in this article, with $\phi \sim 0.1mm$ is non negligible, as the surface area of contact is multiplied by 100 for the same volumic fraction η, which should improve significantly the bonding between fibres and matrix at a material scale. This simple scaling argument is a useful indicator to understand the influence of diameter, but it neglects the fact that bonding quality depends on the fibre scale, because of concrete heterogeneity. For example, the trend observed with concrete rebars in building codes [22] is that the bond quality decreases as the rebar diameter ϕ increases. As such, the argument is a first order approximation of the bond quality between fibres and the mortar.

Another look at this issue, which takes into account the heterogeneity of concrete based on many experiments is the design approach recommended in building codes such as ACI Building Code [23] or Eurocode 2 [22], which proposes a development length that is proportional to the rebar radius in usual

conditions. With good bonding conditions, and proper cover $c_d > 3\phi$, the development length is typically superior to 20ϕ ([22], §8.4.4). If the designers want to comply to the philosophy of these standards, this means that a proper anchorage between reinforcement and mortar can be achieved only if the wall thickness is far superior to the reinforcement diameter. In our case, with fibres of 0.1mm and a wall thickness in the centimetric range, this is clearly achieved. Some experiments are presented in Section 4.3.1 and in a previous publication of the authors in [19].

2.4. First experimentations

In this part, a description of the firsts experiments and observations realised with the prototype device is proposed.

Matrix and reinforcement properties. The matrices are printable mortars designed for robotic extrusion, already at use at the laboratory for full-scale experiments : One is provided by Lafarge (Lafarge NAG3), the other Navier material has been designed at the laboratory (for reference composition see table 1). Reinforcements are Isomatex Filava Conventional Multi-End 400 tex basalt rovings and AGY SCG75 66 tex AR-glass rovings. For more detail see table 2.

Ingredient	Mass proportion
Cement	0.28
Water	0.11
Sand	0.44
Silica fume	0.16
Superplasticizer	0.003

Table 1: Reference composition of the Navier printing mortar.

Roving conveying, fibre impregnation and pulling. Some views of the printing process are presented in the figure 5. 5 bobbins each providing 30 meters of roving are shown on the left view, providing here a fiber ratio of about 0,2%.

Name	Material (-)	Titer (tex)	Density (g/cm^3)	A (mm^2)	f_{fil} (MPa)	E_{fil} (GPa)	ε_{max} (%)
AGY SCG75	AR glass	66	2,48	0,029	3570-3680	87-90	5,7
Isomatex Filava	Basalt	400	2,61	0,154	3400-3700	88-94	2,4

A : Cross-section area of the filament; f_{fil} : tensile strength of the filament; E_{fil} : Tensile modulus of the filament; ε_{max} : ultimate strain.

Table 2: Characteristics of the fibre reinforcement.

Increase this ratio is possible easily using more industrial developments and different layers of bobbins. Another previous attempt with more fibers can be seen in figure 6. Notably, small roving packages are impossible to find due to the lack of industrial applications. These small bobbins are wound from standard bobbins using a custom apparatus permitting a very controlled roll-up, avoiding knots, and minimizing friction. On the right of figure 5 a zoom is made on the printing nozzle, where additives are added and mixed, yarns are impregnated and pulled by the mortar. Schematic view is proposed on figure 4. Yarns are conveyed through PTFE pinholes (1,3), pulleys (2), and inserted in the matrix through a PTFE tube (4). Knowing that the additive effect is time dependant, the yield stress of the concrete matrix increases with time, the output pipe has to be long enough to ensure that the concrete flow becomes sufficiently viscous to pull the fiber. Finally, the resulting anisotropic concrete is extruded out of the nozzle end.

The robotic path is designed here to print square boxes, with different lace thickness. The result of those fibred printing are shown in figure 5. The global good aspect is the proof that the system works rather well. Indeed, due to the process and to the curve shape of the path, any unexpected relative displacement between reinforcement and matrix in the extruded lace should lead to the extraction of the yarn, pulled by the nozzle advance. To better understand this phenomenon, just imagine that a bobbin suddenly stops spinning, due to excessive frictions and insufficient flow shear forces. The consequence will be a tension in the yarn already deposited, and its immediate extraction of the lace. Another key point is that only the shear stress control permits here to negotiate curves correctly, as during a curved path, the inside bend yarns must have a

smaller deposition speed than the outside bend yarns. The modification of the concrete flows inside the nozzle as said before, plays the role of a differential gear.

These first results, obtained with this first laboratory prototype, confirm the rheological analysis and the flow-based pultrusion strategy. The potentialities seem important, and in the next parts we try to explore some of them, both concerning the improvement of the 3d printing process itself and the innovative structural applications it offers.

3. Potential for new extrusion strategies

3.1. Considerations and observations

As mentioned earlier, a key point concerning the robotic extrusion of concrete, is the mastering of the material behavior, yield stress, thixotropy, and its evolution through time. Even for standard horizontal lace deposition patterns, many parameters must be controlled to avoid collapses during deposition, to permit a good bonding between layers (avoid cold joints), to ensure an accurate geometry. For a more complex robotic path, including slopes and cantilever situations the problem will become really tricky and these parameters have no choice but to be real-time adjusted. And to do that, the Oriented Lace Pressing (OLP) is definitely a good alternative to the more classical and frozen Extrusion Lace Shaping (ELS) one. More versatile since real-time adjustable, OLP is however also very sensitive due to the weak yield stress of a more fluid extruded material. Illustrations of these difficulties are shown on figures 7. One can see local and more catastrophic buckling due to a lack of structuration. The material is not able to carry the weight load of the laces above. The reason is a too weak yield stress, locally and at a given time t.

The tuning of the right consistency thanks to - additives - shear stress level (prescribed by the endless screw) - speed of the robotic path - pressures and flow - length of the final pipe of the nozzle - is so , that each non-homogeneity may have consequence. For sure the consistency obtained with ELS technology may

diminish the impact of such defects for a given situation, but once again, this optimisation cannot evolve once the preliminary batch is mixed, prohibiting a more complex printing strategy. A good example of such a need is illustrated in the figure 8. A prototype of a new building system generalizing both concrete printing and masonry principles is proposed (see [26],[27], and next part for details). The concrete laces are extruded on Styrofoam blocks, which serve as thermal insulation in the resulting wall component. The blocks have been removed to display the concrete structure.

The use of polyhedral supports allows complex geometries and sloping deposition of the laces, and a 1.8 meter high concrete truss shown in Figure 8. Despite this encouraging results, the extrusion process requires further improvements to obtain a more controlled aspect. Here the robotic path has ups and downs, crossings, and the rheology has to be time adapted for these different situations. For crossings, due to the local overlapping of several laces, a lower consistency will permit to better spread the different layers and fill the small "expansion tank" specially arranged in the foam. Moreover, printing on slanted supports requires a higher yield stress, as shown analytically in [28]. Based on the equilibrium condition of the lace on the slope, a relation between the angle of this slope and the expected yield stress defines a feasible domain for printing.

To summarize, if the OLP strategy is quite versatile and promising, it appears difficult to change reliably and quickly, from firm to soft, only by the mastering of the matrix physico-chemical composition and reactivity. An alternative is to obtain this evolution through other physical phenomena. It is well known that including fibers in a paste changes its rheological properties, but long fibers have an unusual effect. May have a look now to the figure 9. On the left is an illustration of a classical OLP printing operation, the consistency is quite perfectly adapted to standard printing. One can see the drop formation and its characteristic length, from which the actual yield stress [29] can be identified. On the right figure is a printing of the same material but with only

0,2% of continuous fibers.

The difference is striking: the consistency of the lace permits easy handling and avoids slug effect even though the matrix remains the same. Cold joints are not a problem since the external surface of the lace can be very fluid even though the global firmness is very high. On the right figure 9, a cut is realised. The result can be seen on the right figure 10 showing a very clean slice, impossible to achieve on the fiberless mortar. An interesting perspective for industrial production. On the left figure, another demonstration of the easy handling of the lace, shows the interest of such a technology for very complex printing.

Although the goal of this article is not to propose a fine model of the printing process of fresh anisotropic mortar, a simple model for the mechanical properties of a single fresh lace is proposed in the next section to better understand its potential in the development of new extrusion strategies.

3.2. A simple model for a single fibre-reinforced lace

A homogenised model in elasticity for materials with long rigid inclusions proposed in [30] can be used as a first approximation in order to estimate the longitudinal stiffness and yield stress of a single lace.

3.2.1. Assumptions

This model is based on three hypotheses.

- The ratio between the stiffness of the inclusion and the stiffness of the matrix is high;
- The number of fibers is sufficiently high;
- The volumic fraction η of fibers is close to zero;

The model can be extended to a elasto-plastic model under the assumption of ductility of the materials. These assumptions are all verified for the materials at a young age used in anisotropic concrete extrusion.

Ductility. The considered mortars are ductile materials by design, since this property is required for fiber impregnation. The ductility may be hinted by slug tests for example, as defined and performed in [29] and shown in Figure 9, where striction is clearly visible. Mortar is typically modeled as a Bingham fluid, with a yield stress τ_c and viscosity γ.

The derivation of the simplified model shows that the matrix yields before the fibers, so that the lace has a pseudo-ductile behaviour. However, as the structuration occurs in the mortar, the latter becomes fragile. An elasto-plastic model is thus useful at very early age (typically a few minutes) and is not sufficient to assess the load bearing capacity of printed parts.

Stiffness contrast. The mortar is typically a self-compacting mortar, with a yield stress $\tau_c \sim 200$Pa at the nozzle's tip, and $\tau_c \sim 20$kPa after a few minutes to withstand the weight of the layers without yielding. The elastic modulus E_m depends on the formulation, but a typical ratio is $E_m \sim 10\tau_m$ [31]. The Young's modulus of a glass fiber is 90GPa, several orders of magnitude larger than the one of the cementitious matrix.

Low volumic fraction. Although the continuous fiber alignment allows theoretically for high volumic fractions, practical applications will likely typically require a low amount of fibres. Think of reinforced concrete, where the binding between rebars and concrete is problematic, and where the reinforcement ratio is typically much below 5%. The experiment proposed in this article has a volumic fraction $\eta = 0.2\%$.

3.2.2. Solution

The model [30] assumes a piecewise constant stress field in the fiber and matrix and provides an analytical solution for the case of a uniaxial strain field $\varepsilon_{11} \neq 0, \varepsilon_{22} = \varepsilon_{33} = 0$. The resulting stress fields in the mortar and fibers follow

after the introduction of the Lamé coefficients of the mortar λ_m and μ_m:

$$\underline{\underline{\sigma_m}} \underset{\eta \to 0}{\longrightarrow} \frac{\varepsilon_{11}}{1-\eta} \cdot \begin{pmatrix} \lambda_m + 2\mu_m & 0 & 0 \\ 0 & \lambda_m & 0 \\ 0 & 0 & \lambda_m \end{pmatrix} \tag{5}$$

$$\underline{\underline{\sigma_f}} \underset{\eta \to 0}{\longrightarrow} \varepsilon_{11} \cdot \begin{pmatrix} E_{fiber} & 0 & 0 \\ 0 & 0 & 0 \\ 0 & 0 & 0 \end{pmatrix} \tag{6}$$

Stiffness. The resulting homogenised stiffness E_{eq} is found by summing the contribution of the forces of the mortar and fiber and by dividing by the elongation:

$$E_{eq,\eta} \sim \frac{(1-\eta)\,\sigma_{m,11} + \eta\sigma_{fiber,11}}{\varepsilon_{11}} = \lambda_m + 2\mu_m + \eta E_{fiber} \sim \eta E_{fiber} \tag{7}$$

The stiffness increase is measured by the ratio:

$$\frac{E_{eq,\eta}}{E_0} = 1 + \eta \frac{E_{fiber}}{\lambda_m + 2\mu_m} \tag{8}$$

The evolution of the stiffness function of the volumic fraction of fibers is represented in Figure 11. It appears that the stiffness increase is tremendous, even for small volumic fractions, because the stiffness contrast between the fiber and the fresh mortar is extremely important. The approximation $E_{eq} \sim \eta E_{fiber}$ is thus very good, even for low volumic ratios. It shall also be noticed that the mechanical properties of the mortar rapidly evolve through time (from 200Pa to more than 20KPa), and that the relative benefit of using

Yield stress. Assuming a Von Mises yield criterion for the fresh mortar (citation Coussot), it is possible to find the critical elongation and thus the critical force where the matrix starts to yield. The matrix yields before the fiber if:

$$\frac{E_{fiber}}{\sigma_{fiber}} < \frac{\lambda_m + 2\mu_m}{\tau_c} \tag{9}$$

This hypothesis is verified for the considered material properties. It follows that the yield strain is $\varepsilon_{11} = \frac{\tau_c}{\lambda_m + 2\mu_m}$ and that the equivalent yield stress is given by:

$$\sigma_{c,\eta} = \tau_c \left(1 + \eta \frac{E_{fiber}}{\lambda_m + 2\mu_m}\right) \tag{10}$$

Therefore, the ratio between the relative yield stress increase is equal to the stiffness increase, and the figure 11 does not only represent the evolution of tensile stiffness of a lace, but also the evolution of its equivalent yield stress.

$$\frac{\sigma_{c,\eta}}{\tau_c} = \frac{E_{eq,\eta}}{E_0} \tag{11}$$

3.3. Experimental observations

The simplified model shows that the introduction of a small amount of fibers can drastically modify the longitudinal behaviour. The relative change is much more significant in the fresh state, since the stiffness and strength contrast between the mortar and the fiber is much more important. The figures 9 and 10 illustrate the improvement of longitudinal behavior.

The measure of those changes is however difficult in practice, first because of the magnitude of the evolution introduced by the fibres, second because of the rapid evolution of the mortar after addition of admixtures. The high thixotropy of the mix makes rheometers unusable.

The measure of the apparent yield stress can be done using so-called *slug test* first proposed in [32] for various food industry as "mayonnaise" and recently applied to printable concrete by the authors of the present paper in [19]. This test is based on the study of a cylinder under self-weight, which leads to a catastrophic failure, and the creation of drops or *slugs*. The critical length of a slug can be approximated with equation (12) and depends in first approximation of the yield stress and volumetric weight.

$$H_c = \frac{\sqrt{3}\tau_c}{\rho g} \tag{12}$$

A typical slug length for self-compacting mortar yields slugs of a few centimeters. The slug test formula can be adapted to the anisotropic mortar.

$$H_{c,\eta} = \frac{\sigma_{c,\eta}}{\rho g} \tag{13}$$

Again, Figure 11 illustrates the relative change in slug length. Applying equation (13) with $\eta = 0.2\%$ yields a slug length superior to ten meters, which

cannot be measured in our facilities. Figures 9 right (without fibers) and left (with only 0,2 % of fibers) demonstrate quite well this "apparent yield stress" improvement, and the new opportunities.

3.4. Potentials during printing stages

The high tensile strength of the fresh lace surely offers potential for new applications in concrete printing. In particular, although 3d printing is often presented as a technology that offers seemingly limitless formal possibilities without the need for any formwork, the printing of concrete structures without scaffolding remains an open research question [25]. Practical limitations appear indeed very quickly because of the poor tensile capacity of mortar. To illustrate this statement, we consider an intermediate stage in the 3d printing of an arch, as shown in Figure 12. The tensile force H, the arch compression force C, the slope angle α and line weight w are related by the equations of equilibrium (14).

$$\begin{cases} H = \dfrac{w}{\tan\alpha} \\ C = \dfrac{w}{\sin\alpha} \end{cases} \tag{14}$$

Thus, tensile strength limits the cantilevering possibilities without reinforcement since H and C have the same order of magnitude.

Anisotropic concrete could therefore offer a tremendous potential for the printing of cantilever. Figure 14a shows the printing sequence of an arch and its influence on the tensile force (and therefore the need for reinforcement). The tensile stress increases until the arch is completed. The structure is then funicular and the reinforcement is not needed anymore (or to a much lesser extent). This opens the route to the use of natural fibers, which face durability issues without proper treatment [33], but that could perfectly be used as eco-friendly reinforcement during printing of supportless structures. This proposition is illustrated in Figure 14b, where the natural fibers tend to naturally decay in a few months or years: notice that the time scale is not linear, as the decay of natural fibres in concrete is several orders of magnitude larger than the printing time.

4. Potential for new structural applications

In the previous part, a focus was made on the printing process itself and on the direct interest of a continuous lace reinforcement in the context of an OLP strategy. Even a poor ratio of fibres drastically affects the mechanical behaviour of fresh laces. This rheological change may offer great comfort and reliability of the flow deposition process. The next step, of course, is to imagine which new opportunities *anisotropic concrete* may offer to structural applications.

4.1. Anisotropy in reinforced concrete structures

Fiber-reinforced concrete are essentially used as isotropic materials, or with little anisotropy. Indeed, Fibre-Reinforced Ultra-High Performance Concrete is usually isotropic, because fibres are in the concrete mix before casting. Fibre orientation is however possible through the control of the flow [34], or through other means, like electromagnetic fields.

Isotropy provides ductililty in any direction, which is surely of interest for thin-walled structures, which can be subject to punch-shear failures or accidental loads. However, the design philosophy of reinforced concrete is historically based on its composite action, and on a strong anisotropy. The strut-and-tie method, which has been popularised by Schlaich [35], is used in the ACI Building code since 2002 and Eurocode 2. This method proposes to evaluate the load-bearing capacity of reinforced concrete by postulating a stress field at equilibrium satisfying the yield criterion of the materials at stake: it can thus be seen as a particular case of the lower-bound theorem in the yield design theory. The stress fields in strut-and-tie models are singular, with compressive struts in concrete, while the rebars are associated with ties in tension. They reflect thus a truly anisotropic behaviour. Example of strut-and-tie model for a corbel is shown in Figure 15. The model of Figure 15b is more complex than the one of Figure 15a, but also uses less material. Nevertheless, simple models are preferred over complex mechanical optima because they are more economical.

Some efficient strut-and-ties models and thus rebar configurations are known, but are not used in practice due to the labour cost for their fabrication. A first application of the anisotropic concrete proposed in the present article can be to make more complex scheme for ties in massive structures, replacing rebars.

4.2. Filigree concrete structures

The strut-and-tie method should be understood as a simplification of yield design theory, where one looks for a stress field at equilibrium satisfying the yield criterion everywhere. One could argue that this remains a theoretical method without constructive rationality. However, while monolithic concrete structures are now ubiquitous, a study of historical structures shows that uni-axial stress fields in reinforced concrete structures are possible, and were actually the norm when material was still more expensive than human labour. For example, the famous Chiasso Shed, designed by Swiss engineer Robert Maillart, [36] and shown in Figure 16 was designed as a constant stress structure. The strut-and-tie model coincides with the structural shape, making a visually striking embodiment of the idea of structural form. The efficiency of the design compared to common concrete structure is undeniable.

A detail shown in Figure 17. The image reveals the delicacy of the structure, but also its complexity, especially if one thinks of formwork. Here, an additive manufacturing technology such as the proposed anistropic concrete could allow for the the construction of highly efficient structures, without any kind of formwork and thus the waste or cost associated [38].

Finally, it shall be noted that the strut-and-tie approach has some connections to optimal structural design, like optimal truss analytically described by Michell [39]. Later, inspiration from Michell truss have lead to numerical methods for the structural optimisation of continuum media [40]. It can be argued that optimal solutions in mechanical problems are related to the anisotropy at the material scale. For example, the homogenisation method introduces microstructure inspired by laminated composites to regularise the topology optimisation [41]. Therefore, anisotropic concrete can be viewed as a way to materialise

mechanically optimal structures in a more general sense, by controlling local anisotropy and allowing designers to put *the right material at the right place*. This requires however a design approach inspired by composite material and multi-layer structures. This is perhaps where anisotropic concrete provides its greatest potential for structural applications.

4.3. Think composite

The real novelty of *anisotropic concrete* is that even if the mix of the material is well-known (cementitious matrix plus fibers from any sort) the fibers arrangement and the resulting mechanical properties are rather unusual to the civil engineering community. Here the fibers are assembled in continuous yarns and aligned only in the longitudinal direction, conferring the claimed anisotropy, and the opportunity to include a high volumic ratio of fibers as in figure 18.

This kind of matrix and fibers arrangement is called Fiber Reinforced Material (FRM) or FRP when designed with a polymeric matrix as epoxy or polyester. Today FRPs are very usual for a large part of the other industrial sectors as aeronautics, transportation, sports and leisure. Considering cementitious as a ceramic, it even exists already continuous fibre ceramic matrix composites for very high-performance applications, especially when high temperature and stiffness are required, for engine applications or more recently in future nuclear reactors [42]. This class of material FRM postulates generally high longitudinal mechanical characteristics (those from fibers) which discriminates it from more standard composites reinforced with small fibers randomly distributed. The anisotropic concrete we propose here claims to belong to this family. For now it differs a little bit since the ratio of longitudinal reinforcement is far from the expected ratio that can be found in classical unidirectional composites. We have detailed above our first experimentation involving a few percent per volume, when 60% can be achieved for FRP. But it doesn't seem to be a problem to increase drastically this ratio until 10% or more, if an industrial device is designed. But another important aspect concerning the *DNA* of the FRM is perhaps more than the ratio of fibers, the quality of the assembly, the way the

fibers are mechanically connected with the matrix, the efficiency of their interfaces. The synergy is only possible if the stress transfer from shear in the matrix to tensile in fibers is ensured. In this case the material can be considered as homogeneous and an equivalent behavior defined. Here, due to aligned fibers, the right term is *transverse isotropic* behavior. If it's the case, then we can start to *think composite*.

4.3.1. Transverse isotropic behavior

In another paper [19] a focus is made on the interface quality characterisation. This is a prerequisite aspect, if a mechanical design has to be done. In the case of a reinforcement using multi-fiber yarns, such as the one used in this work, the impregnation of the yarn had a great influence on the interfacial bond as demonstrated in [43]: a better impregnation lead to a higher interfacial strength. To better understand the interfacial behavior in our own application, tension stiffening tests (kind of pull-out tests) and in-situ intensive tomographic observations, were made [19]. Single multi-fiber yarns embedded in millimetric prismatic specimens of mortar are used. In figure 21 a microtomographic view shows a yarn embedded in the matrix during an in-situ tension test.

A globally good impregnation seems to be achieved, with the finest cementitious part migrated inside the yarn. Moreover, crack patterns reveal a good mechanical transfer between fibers and matrix, due to a good interface: 45° angle in the matrix testifies for high shear, and the horizontal transverse cracks inside the yarn for tension. Exactly what the continuum mechanics predicts for a good composite material. Figure 20 shows the force versus strain curve for different formulations and fibers. The stiffness of the composite appears higher than the stiffness of the isolated yarn, and the interface ensures a good elastic transfer until 0,5%. After that, depending on the fiber-matrix couple, more or less ductility is exhibited. This reflects a progressive damage of the interface. Finally when all the interface is destroyed, the stiffness of the fiber is recovered. More details may be found in [19].

Finally, for the reinforced material, a transverse isotropic behavior may be

assumed with a compliance S as:

$$S = \begin{pmatrix} 1/E_l & -\nu_{lt}/E_l & -\nu_{lt}/E_l & 0 & 0 & 0 \\ -\nu_{lt}/E_l & 1/E_t & -\nu_{ln}/E_t & 0 & 0 & 0 \\ -\nu_{lt}/E_l & -\nu_{ln}/E_t & 1/E_t & 0 & 0 & 0 \\ 0 & 0 & 0 & 2\frac{1+\nu_{ln}}{E_t} & 0 & 0 \\ 0 & 0 & 0 & 0 & 1/G_{lt} & 0 \\ 0 & 0 & 0 & 0 & 0 & 1/G_{lt} \end{pmatrix} \tag{15}$$

with E_l,E_t the longitudinal and transverse young moduli, ν_{lt} and ν_{tn} the two Poisson ratios and G_{lt} the shear modulus in the lt plane.

Thanks to the tests and observations above on figure 21, we may now assume an equivalent homogeneous material, and these 5 moduli may be estimated by very simple rule of mixture formulas deriving from continuum mechanics. For instance, assuming that the axial fibre strain is equal to the matrix axial strain (in the elastic phase), a Voigt description can be used for E_l estimation:

$$E_l = fE_f + (1-f)E_m \tag{16}$$

with f the volumic ratio of fibers, E_f and E_m the longitudinal young moduli of fiber and matrix.

Considering matrix and fibers as defined in tables 1 and 2, (mean values about respectively 20 GPa and 90GPa for Young moduli), the linear dependency with a f between 0% and 40%, gives a E_l variation between 20 and 48 GPa. 40% is quite a lot, even if obtained for ceramic composites. The expected maximum value for flow-based pultrusion proposed here, is more about 10%, giving $E_l = 27\,GPa$, meaning an expected increasing of 35% for the axial modulus. For a ratio of fibers about 5% and 1%, 17% and 3,5% are respectively obtained. It seems weak, but for a standard reinforced concrete beam for example, Eurocode prescribes a maximum of 4% of steel bending rebars per volume, to limit the steel quantity and the ensure a casting feasibility and quality. A usual ratio for civil engineering is 180 kg/m3 of steel, meaning 2-3% per volume, including

all the rebars (bending and shear), and rather 1.5% for buildings. Focusing on buildings, considering a stiffness criteria and a steel Young modulus twice of those of glass and basalt fibers, it gives 3% for mineral yarns to replace rebars. Considering also that the steel rebars are more concentrated in the tensed area of the beam, 6-10% is rather to target and possible from a technological point of view.

However stiffness is not the only aspect to consider. The great interest of this distributed longitudinal reinforcement concerns more the improvement of the limit state, resistance, and ductility. To understand and quantify these aspects cast *model* tension specimens are tested. The challenge is to propose ideal specimens representative of the printed process, but with a more controlled fiber distribution permitting mechanical studies. Details will be published soon but first attempts in [18] already highlighted the expected interest concerning the ultimate behavior of the anisotropic concrete. On the right of the figure 22 a Force-Strain graph depicts the strain-hardening behaviour until rupture. Such ductility for tension is only due to fibers and to the progressive microcracking on matrix, materialized by jumps on the curve. On the left, such a multiple crack pattern is highlighted in red, characteristic of a tensed reinforced concrete.

Several applications may be imagined using this anisotropic concrete. The proposal of [27] and reported on figure 8 is a good example, as in a truss, bars are only submitted to tension and compression. As said before, this transverse isotropic material may also be interesting to help for bending and cantilever situation as in tensed rings of the corolla's upper part shown on Figure 13).

4.3.2. Cross-plies and multilayers

A second step is naturally to investigate the usual way composite are used in industry. The unidirectional case, if the simplest way to achieve an anisotropic behavior, is not the most common one and very often unidirectional (transversely isotropic) layers are stacked with different angles to constitute cross-plies. The angles are optimised to carry the different loading the structure

should endure. The anisotropic concrete may permit such a strategy. For orthotropic slabs, it becomes possible to provide the stiffness in both directions by the printing in the two directions (figure 23). Multilayer's strategy is also an alternative if the bending stiffness is required, and the usual answer is the sandwich architecture. A light core ensures the stress transfer between two stiff skins, and the combo proposes a ratio inertia/weight very interesting for bending (figure 23). Naturally, skins, here unidirectional, may be cross-plies. Moreover, with 3d Printing, the shape is no more a problem, and curve panels can be easily achieved. Note that the core may also be a printed light concrete.

Mainly used for manufacturing open (cylinders) or closed-end structures (pressure vessels or tanks), this manufacturing technique involves winding filaments under tension over a rotating mandrel, laying down fibers in the desired pattern or angle. Comparing to steel, usually used for this kind of structure, winding materials provide much lighter pressurized structures. But a more ductile behavior is also achieved thanks to the fibers which avoid brutal propagation of the first crack at the critical pressure. This technique can be really taylor made also for the anisotropic concrete. Especially for big pipes or tanks and when steel or polymeric materials are not allowed (as for nuclear wastes) or have to be protected against corrosion. It's the case for submarine steel pipelines which usually have a continuous concrete 'coating' applied to give weight (for stability under ocean currents) and mechanical protection to the corrosion protection coating [44] as shown in the right figure 24.

5. Conclusion

First real-scale concrete realizations involving additive manufacturing have been achieved in the past decades. It seems impossible now that these new digital technologies will not be a part of the toolkit for tomorrow's building. The main gap between experimentation and industry is probably that printed components are not reinforced, and do not yet comply with building standards or basic reliability principles. Consequently they are not used as load-bearing

components and not yet in the competition. Actually, despite several attempts, no industrial solution for the reinforcement of the 3D printed components exist. This article presents a patented solution for reinforcement of 3D printed structures. Inspired by the composite industry it is called *flow-based pultrusion for additive manufacturing*. A strict control of the rheological behaviour of the cementitious matrix ensures the routing and impregnation of continuous yarns of thin fibres resulting to an *Anisotropic Concrete*. Homogeneously reinforced in a single direction, the material proposes enhanced strength and ductility. This paper describes the process, its constraints, and first experimental achievements.

Thanks to the possibility of a better mastering of the time-dependent rheology of the mortar, Oriented Lace Pressing (OLP) technology is chosen as may combine, first a good impregnation of yarns and then, a good mechanical behavior of the stacking of printed laces. Another point is that only the shear interaction between the concrete flow and the yarns ensures the pulling force on the yarns avoiding any external motorization and helping to "natural" management of the fiber deposition, especially in the curve parts of the path when each fiber must have a different speed to fit the nozzle trajectory. A nozzle prototype on an OLP printing device, 5 bobbins of glass and basalt fibers, and a printable mortar are used, providing a fiber ratio between 0,2% and 1%. Increasing this ratio is easily possible using more bobbins and industrial developments. Printings with different curvatures and lace thickness present a global good aspect, proof the efficiency of the system.

These experiments highlight new possibilities about the process itself as the consistency of the lace, even with few fibers, permits a more easy handling and avoids avalanche and slug effects during the printing. A simple mechanical model explain this important and unexpected issue.

New constructive solutions and structural applications are finally imagined. Some of them are inspired by famous architectural concrete designs, playing with anisotropy, struts and ties mechanics, some others derive directly from the composite material industry as cross-plies and sandwiches structures for a new design of tanks and orthotropic concrete panels.

Acknowledgment

This work was made in the framework of Nicolas Ducoulombier and Leo Demont's PhD theses. Nicolas Ducoulombier's thesis is funded by LABEX MMCD. Leo Demont's thesis is funded by Ecole des Ponts ParisTech and Build'in, a technology platform of its Co-Innovation Lab. The authors also acknowledge the fruitful collaboration with XTreeE, technology provider of the extruder and HAL Robotics for joined software development for robotic control.

References

[1] E. Worrell, L. Price, N. Martin, C. Hendriks, L. O. Meida, Carbon dioxide emissions from the global cement industry, Annual Review of Energy and the Environment 26 (1) (2001) 303–329. doi:10.1146/annurev.energy.26.1.303.

[2] R. M. Andrew, Global co2 emissions from cement production, Earth Syst. Sci. Data 10 (2018) 195–217.

[3] A. Nanni, Flexural behavior and design of rc members using frp reinforcement, Journal of structural engineering 119 (11) (1993) 3344–3359. doi:https://doi.org/10.1061/(ASCE)0733-9445(1993)119:11(3344).

[4] O. Chaallal, B. Benmokrane, Fiber-reinforced plastic rebars for concrete applications composites, Part B: Engineering 27 (3-4) (1996) 245–252. doi:https://doi.org/10.1016/1359-8368(95)00023-2.

[5] K. Benzarti, X. Colin, Understanding the durability of advanced fibre-reinforced polymer (frp) composites for structural applications, in: W. publishing Series (Ed.), Advanced Fibre-Reinforced Polymer (FRP) Composites for Structural Applications, Civil and Structural Engineering, 2013, Ch. 12, pp. 361–439.

[6] J. Hegger, S. Voss, Investigations on the bearing behaviour and application potential of textile reinforced concrete, Engineering Structures 30 (7) (2008) 2050–2056. doi:https://doi.org/10.1016/j.engstruct.2008.01.006.

[7] C. Pascal, P. Rossi, I. Schaller, Can steel fibers replace transverse reinforcements in reinforced concrete beams?, Materials Journal 94 (5) (1996) 341–354.

[8] S. Lim, R. A. Buswell, T. T. Le, S. A. Austin, A. G. F. Gibb, T. Thorpe, Developments in construction-scale additive manufacturing processes, Automation in Construction 21 (2012) 262–268. doi:10.1016/j.autcon.2011.06.010.

[9] G. Vantyghem, W. De Corte, E. Shakour, O. Amir, 3D printing of a post-tensioned concrete girder designed by topology optimization, Automation in Construction 112 (2020) 103084. doi:10.1016/j.autcon.2020.103084.

[10] D. Asprone, C. Menna, F. P. Bos, T. A. M. Salet, J. Mata-Falcón, W. Kaufmann, Rethinking reinforcement for digital fabrication with concrete, Cement and Concrete Research 112 (2018) 111–121. doi:10.1016/j.cemconres.2018.05.020.

[11] E. Lloret, A. Shahab, M. Linus, R. Flatt, F. Gramazio, M. Kohler, S. Langenberg, Complex concrete structures: Merging existing casting techniques with digital fabrication, Computer-Aided Design 60 (2015) 40–49. doi:https://doi.org/10.1016/j.cad.2014.02.011.

[12] SF3DR, 3 dr ® structural formwork (1999).
URL https://www.3drcoffrages.com/en/

[13] Z. Ren, L. Wang, Applied research of light steel rib-concrete with dipy construction formwork system, Proceedings of the Fourth International Conference on Advances in Steel Structures I (2005) 665–670. doi:https://doi.org/10.1016/B978-008044637-0/50097-4.

[14] B. Khoshnevis, D. Hwang, K.-T. Yao, Z. Yah, Mega-scale fabrication by contour crafting, Int. J of Industrial and Systems Engineering 60 (2006) 301–320. doi:http://dx.doi.org/10.1504/IJISE.2006.009791.

[15] F. P. Bos, Z. Y. Ahmed, E. R. Jutinov, T. A. M. Salet, Experimental Exploration of Metal Cable as Reinforcement in 3D Printed Concrete, Materials (Basel, Switzerland) 10 (11) (Nov. 2017). doi:10.3390/ma10111314.

[16] M. Hambach, D. Volkmer, Properties of 3d-printed fiber-reinforced portland cement paste, Cem. Concr. Compos. 79 (2017) 62–70. doi:http://dx.doi.org/10.1016/j.cemconcomp.2017.02.001.

[17] B. Panda, P. Chandra, M. Jen Tan, Anisotropic mechanical performance of 3d printed fiber reinforced sustainable construction material, Material Letters. 209 (2017) 146–149. doi:http://dx.doi.org/10.1016/J.MATLET.2017.07.123.

[18] N. Ducoulombier, L. Demont, C. Chateau, M. Bornert, J. Caron, Additive manufacturing of anisotropic concrete: a flow-based pultrusion of continuous fibers in a cementitious matrix, Procedia Manufacturing 47 (2020) 1070–1077.

[19] N. Ducoulombier, C. Chateau, M. Bornert, J.-F. Caron, P. Aimedieu, T. Weitkamp, J. Perrin, A. King, M. Scheel, X-ray tomographic observations of microcracking patterns in fibre-reinforced mortar during tension stiffening tests, Strain (2020).

[20] C. Gosselin, R. Duballet, N. Roux, Ph.and Gaudillière, J. Dirrenberger, P. Morel, Large-scale 3d printing of ultra-high performance concrete – a new processing route for architects and builders, Materials Design 100 (2016) 102–109. doi:https://doi.org/10.1016/j.matdes.2016.03.097.

[21] N. Roussel, A thixotropy model for fresh fluid concretes: Theory, validation and applications, Cement and Concrete Research 36 (2016) 1797–806. doi:https://doi:10.1016/j.cemconres.2006.05.025.

[22] Eurocode 2 - design of concrete structures: part 1-1 -general rules and rules for buildings, BSI, London, 2004.
URL https://cds.cern.ch/record/1745970

[23] ACI, Aci 318-11 building code requirements for structural concrete (2011).

[24] N. Gaudillière, R. Duballet, C. Bouyssou, A. Mallet, P. Roux, M. Zakeri, J. Dirrenberger, Large-Scale Additive Manufacturing of Ultra-High-Performance Concrete of Integrated Formwork for Truss-Shaped Pillars, in: Robotic Fabrication in Architecture, Art and Design 2018, Springer International Publishing, 2018, pp. 459–472. doi:10.1007/978-3-319-92294-2_35.
URL https://hal.archives-ouvertes.fr/hal-01904661

[25] P. Carneau, R. Mesnil, N. Roussel, O. Baverel, Additive manufacturing of cantilever - from masonry to concrete 3d printing, Automation in Construction (2020).

[26] R. Duballet, Systèmes constructifs en fabrication additive de matériaux cimentaires, Ph.D. thesis (Sep. 2019).

[27] R. Duballet, O. Baverel, J. Dirrenberger, Space truss masonry walls with robotic mortar extrusion, Structures 18 (2019) 41–47.
URL https://hal.archives-ouvertes.fr/hal-02089858/document

[28] R. Duballet, R. Mesnil, N. Ducoulombier, P. Carneau, L. Demont, Motamedi, O. Baverel, J.-F. Caron, J. Direnberger, Free deposition printing for space truss structures, in: Second RILEM International Conference on Concrete and Digital Fabrication – Digital Concrete 2020, 2020.

[29] N. Ducoulombier, P. Carneau, R. Mesnil, J.-F. C. Caron, R. Roussel, "the slug test": Inline assessment of yield stress for ex-trusion-based additive manufacturing, in: Second RILEM International Conference on Concrete and Digital Fabrication – Digital Concrete 2020, 2020.

[30] P. de Buhan, J. Bleyer, G. Hassen, 3 - macroscopic behavior of materials reinforced by thin highly stiff/resistant linear inclusions, in: P. [de Buhan], J. Bleyer, G. Hassen (Eds.), Elastic, Plastic and Yield Design of Reinforced Structures, Elsevier, 2017, pp. 93 – 151. doi:https://doi.org/10.1016/B978-1-78548-205-2.50003-7.
URL http://www.sciencedirect.com/science/article/pii/B9781785482052500037

[31] A. Suiker, Mechanical performance of wall structures in 3d printing processes: Theory, design tools and experiments, International Journal of Mechanical Sciences 137 (2018) 145 – 170. doi:https://doi.org/10.1016/j.ijmecsci.2018.01.010.
URL http://www.sciencedirect.com/science/article/pii/S0020740317330370

[32] P. Coussot, F. Gaulard, Gravity flow instability of viscoplastic materials: The ketchup drip, Phys. Rev. E 72 (2005) 031409. doi:10.1103/PhysRevE.72.031409.
URL https://link.aps.org/doi/10.1103/PhysRevE.72.031409

[33] G. Ramakrishna, T. Sundararajan, Studies on the durability of natural fibres and the effect of corroded fibres on the strength of mortar, Cement and Concrete Composites 27 (5) (2005) 575 – 582, natural fibre reinforced cement composites. doi:https://doi.org/10.1016/j.cemconcomp.2004.09.008.
URL http://www.sciencedirect.com/science/article/pii/S0958946504001489

[34] P. Stähli, R. Custer, J. G. van Mier, On flow properties, fibre distribution, fibre orientation and flexural behaviour of frc, Materials and structures 41 (1) (2008) 189–196.

[35] J. Schlaich, K. Schafer, Design and detailing of structural concrete using strut-and-tie models, Structural Engineer (6) (1991) 113–125.

[36] R. Mark, J. K. Chiu, J. F. Abel, Stress analysis of historic structures: Maillart's warehouse at chiasso, Technology and Culture (1974) 49–63.

[37] D. Zastavni, The structural design of maillart's chiasso shed (1924): a graphic procedure, Structural Engineering International 18 (3) (2008) 247–252.

[38] F. Antony, R. Grießhammer, T. Speck, O. Speck, Sustainability assessment of a lightweight biomimetic ceiling structure, Bioinspiration & Biomimetics 9 (1) (2014) 016013. doi:10.1088/1748-3182/9/1/016013.

[39] A. G. M. Michell, LVIII. the limits of economy of material in frame-structures, The London, Edinburgh, and Dublin Philosophical Magazine and Journal of Science 8 (47) (1904) 589–597. doi:10.1080/14786440409463229.

[40] G. Strang, R. V. Kohn, Hencky-prandtl nets and constrained michell trusses, Computer Methods in Applied Mechanics and Engineering 36 (2) (1983) 207 – 222. doi:https://doi.org/10.1016/0045-7825(83)90113-5.

[41] G. Allaire, F. Jouve, H. Maillot, Topology optimization for minimum stress design with the homogenization method, Structural and Multidisciplinary Optimization 28 (2-3) (2004) 87–98.

[42] C. Chateau, L. Gélébart, M. Bornert, J. Crépin, D. Caldemaison, C. Sauder, Modeling of damage in unidirectional ceramic matrix composites and multi-scale experimental validation on third generation SiC/SiC minicomposites, Journal of the Mechanics and Physics of Solids 63 (2014) 298–319. doi:10.1016/j.jmps.2013.09.001.

[43] X. Zhang, H. Aljewifi, J. Li, Failure mechanism investigation of continuous fibre reinforced cementitious composites by pull-out behaviour analysis, Procedia Mater Sci 3 (2014) 1377—-1382. doi:https://doi.org/10.1016/j.mspro.2014.06.222.

[44] P. Smith, 2 - types of marine concrete structures, in: M. G. Alexander (Ed.), Marine Concrete Structures, Woodhead Publishing, 2016, pp. 17 – 64. doi:https://doi.org/10.1016/B978-0-08-100081-6.00002-7.
URL http://www.sciencedirect.com/science/article/pii/B9780081000816000027

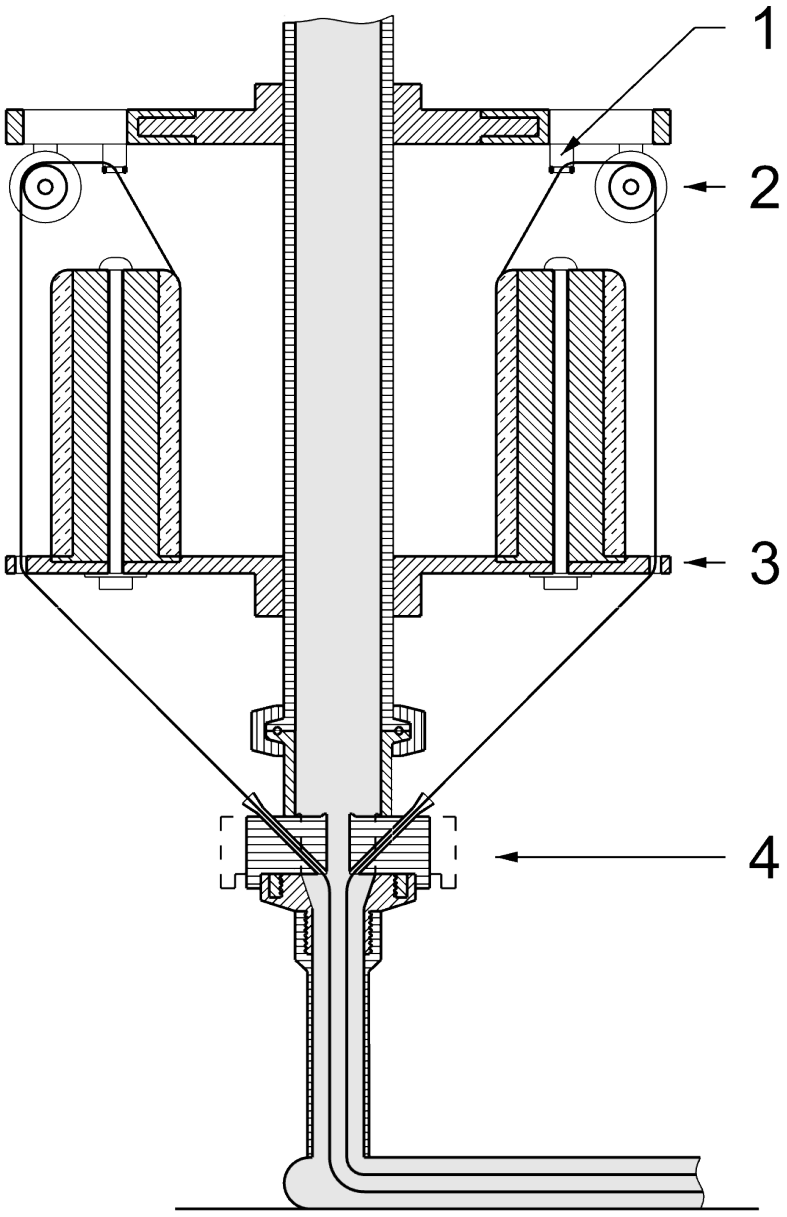

Figure 4: Section of the experimental device.

Figure 5: 3d printing of anisotropic concrete.

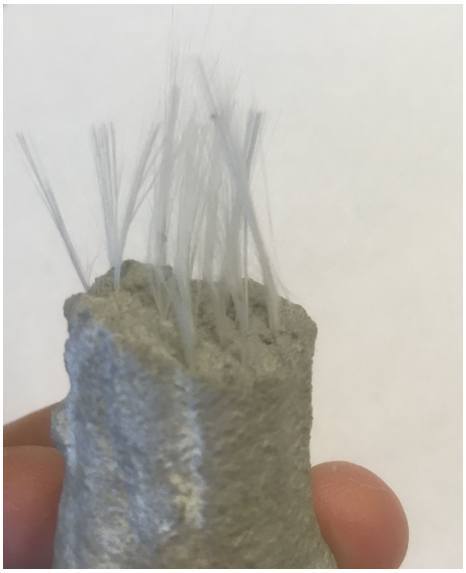

Figure 6: Lace with 1% fiber by volume.

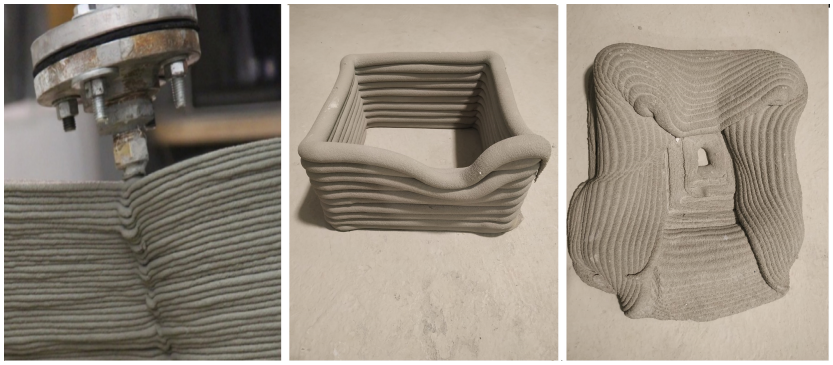

Figure 7: Local and global defects due to a lack of consistency during OLP printing (the left view from [24], right view from [25])

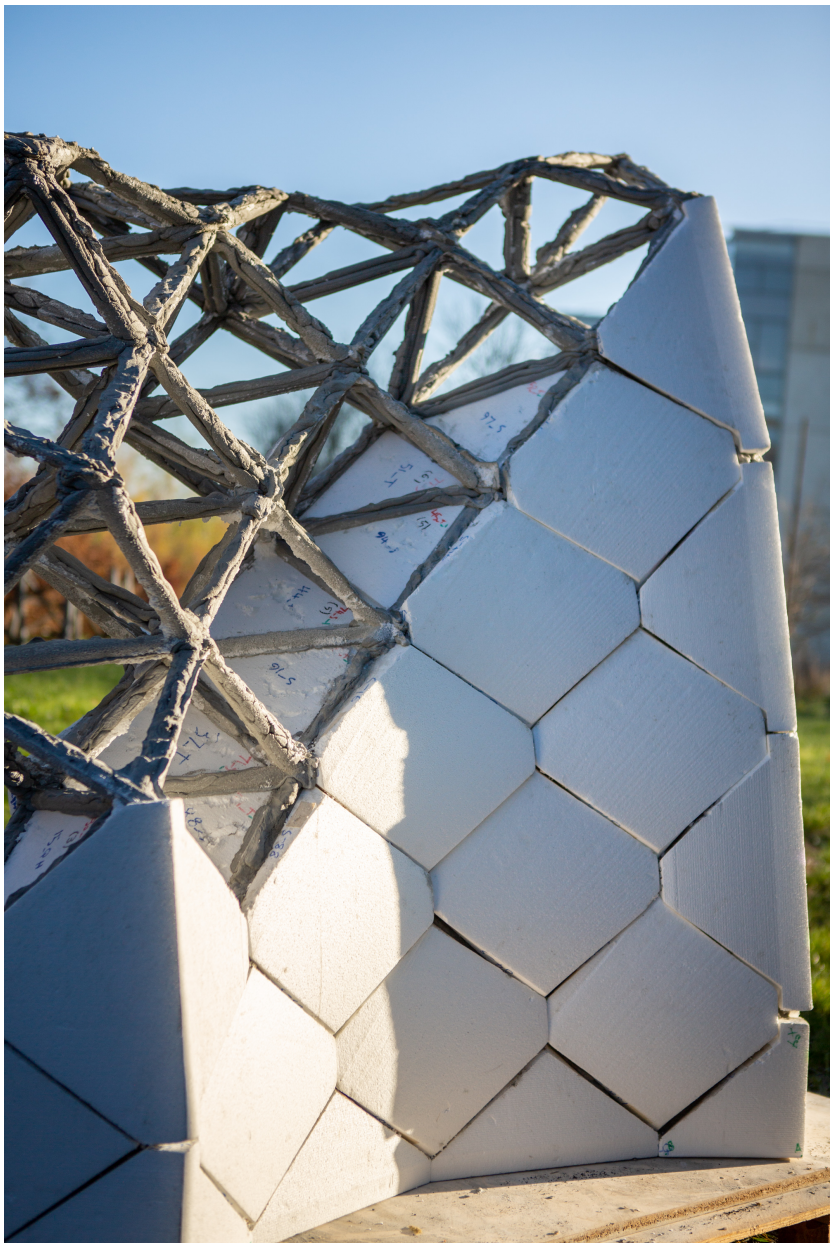

Figure 8: Space Truss Masonry Wall with Robotic Extrusion [27, 28]

Figure 9: Lace behavior without (left) and with 0,2% fiber by volume (right) - same cement formulation.

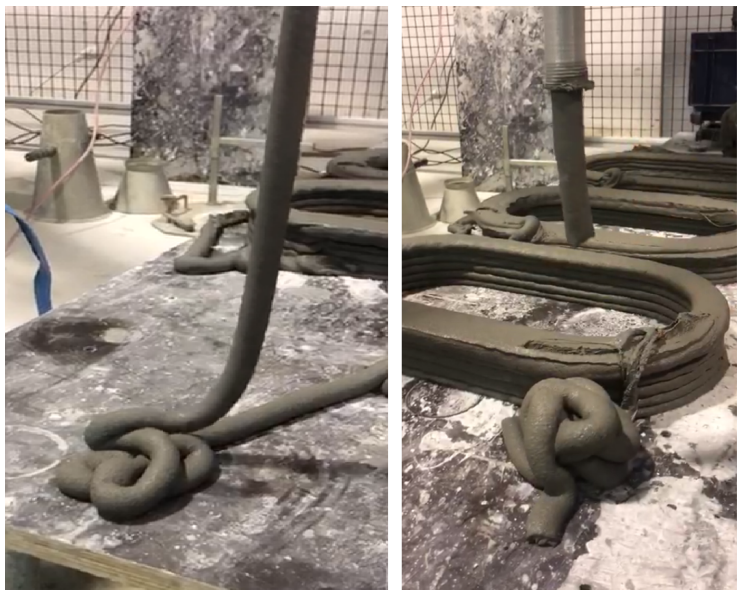

Figure 10: easy-handling of a lace with 0.2% fiber by volume, and sharp result of a cissor cut.

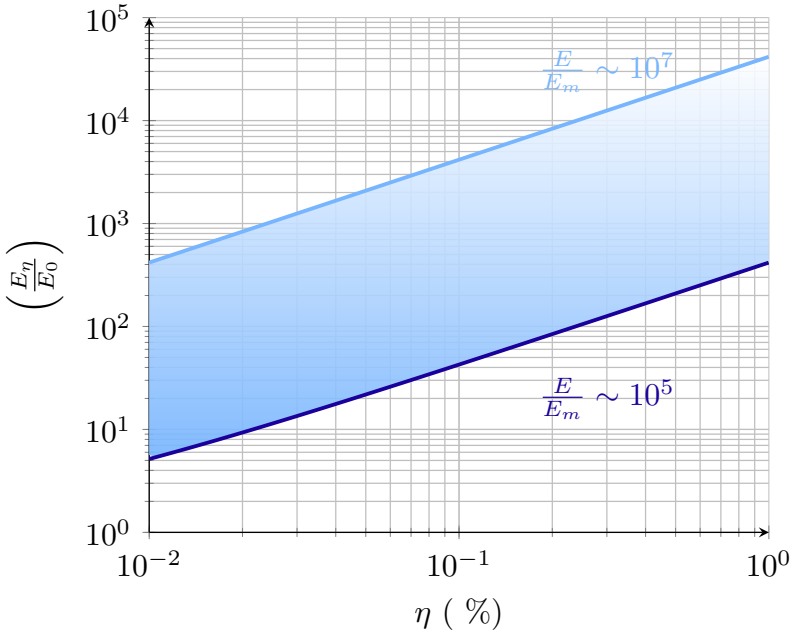

Figure 11: Evolution of tensile stiffness of a fresh lace with respect to the volumic fraction η.

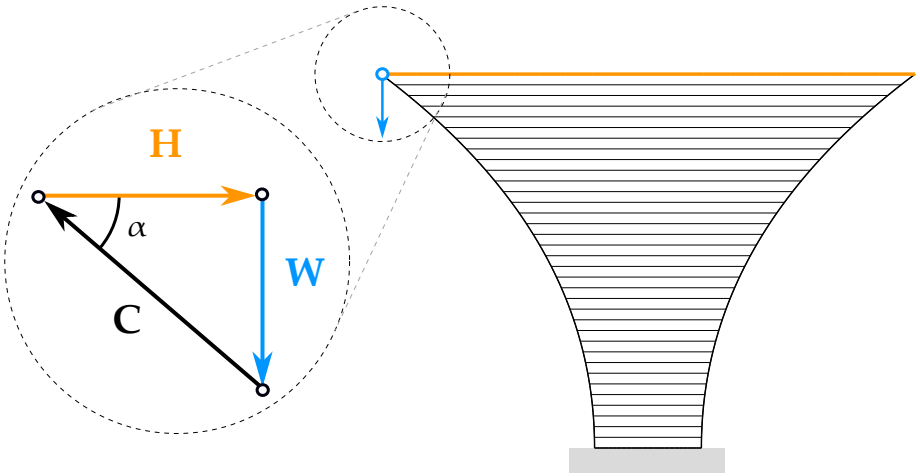

Figure 12: Equilibrium of a cantilevering arch (or corolla). The equilibrium is represented through a Cremona diagram.

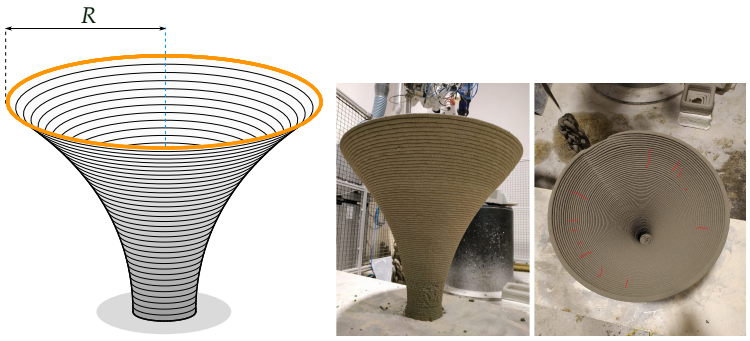

Figure 13: Corolla and cracking pattern in tensed rings

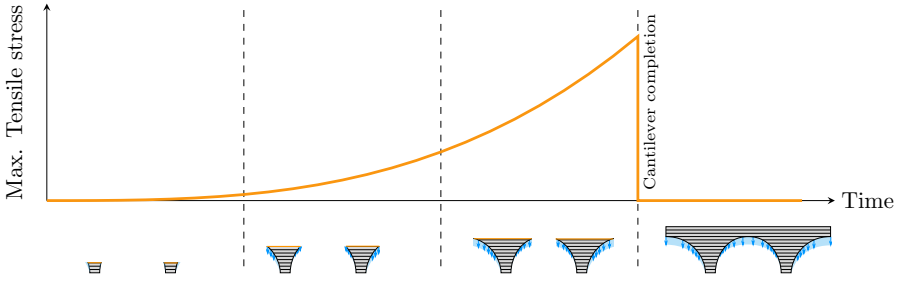

(a) Construction sequence of an arch without scaffolding and resulting tensile stress.

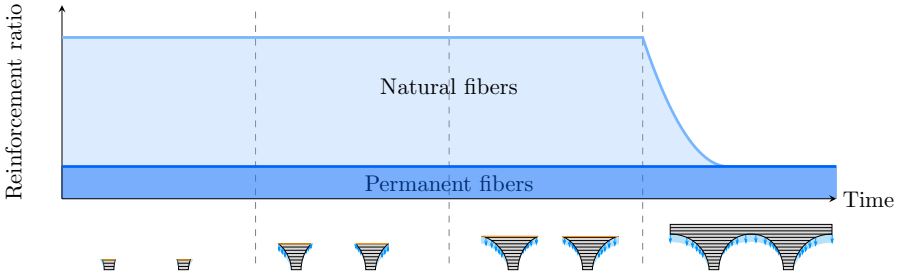

(b) Proposition for a mix of permanent and natural fibers to improve the construction of cantilevers.

Figure 14: Construction sequence of cantilevers and proposal for reinforcement strategy.

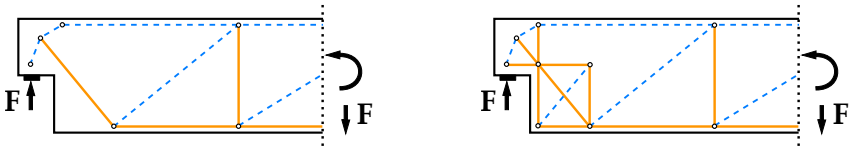

(a) Simple model.

(b) Complex model.

Figure 15: Strut and tie method for a corbel, after [35]. Struts are shown in dashed lines, ties (corresponding to reinforcements) are shown in thick orange lines.

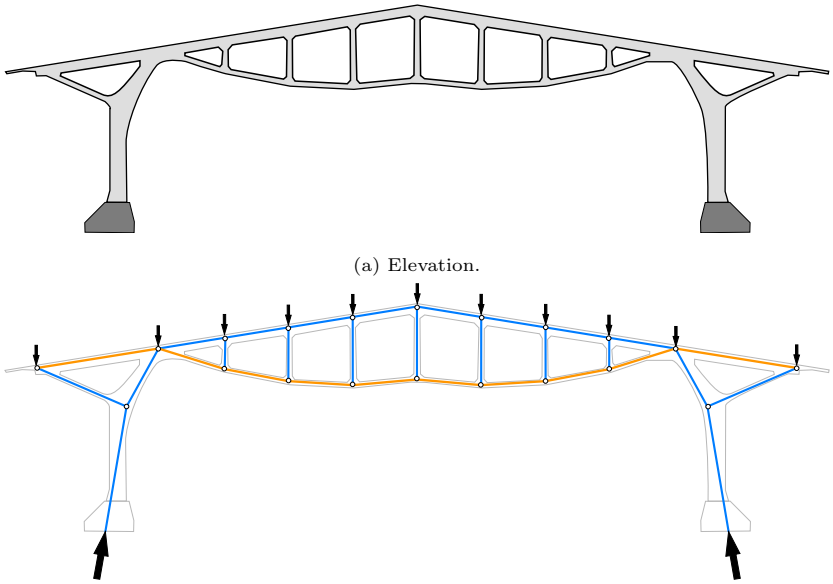

(a) Elevation.

(b) Strut-and-tie model.

Figure 16: Chiasso Shed: a filigree concrete structure, after [37].

Figure 17: Close-up on the Chiasso Shed structure, by Robert Maillart (picture: Mark [36]).

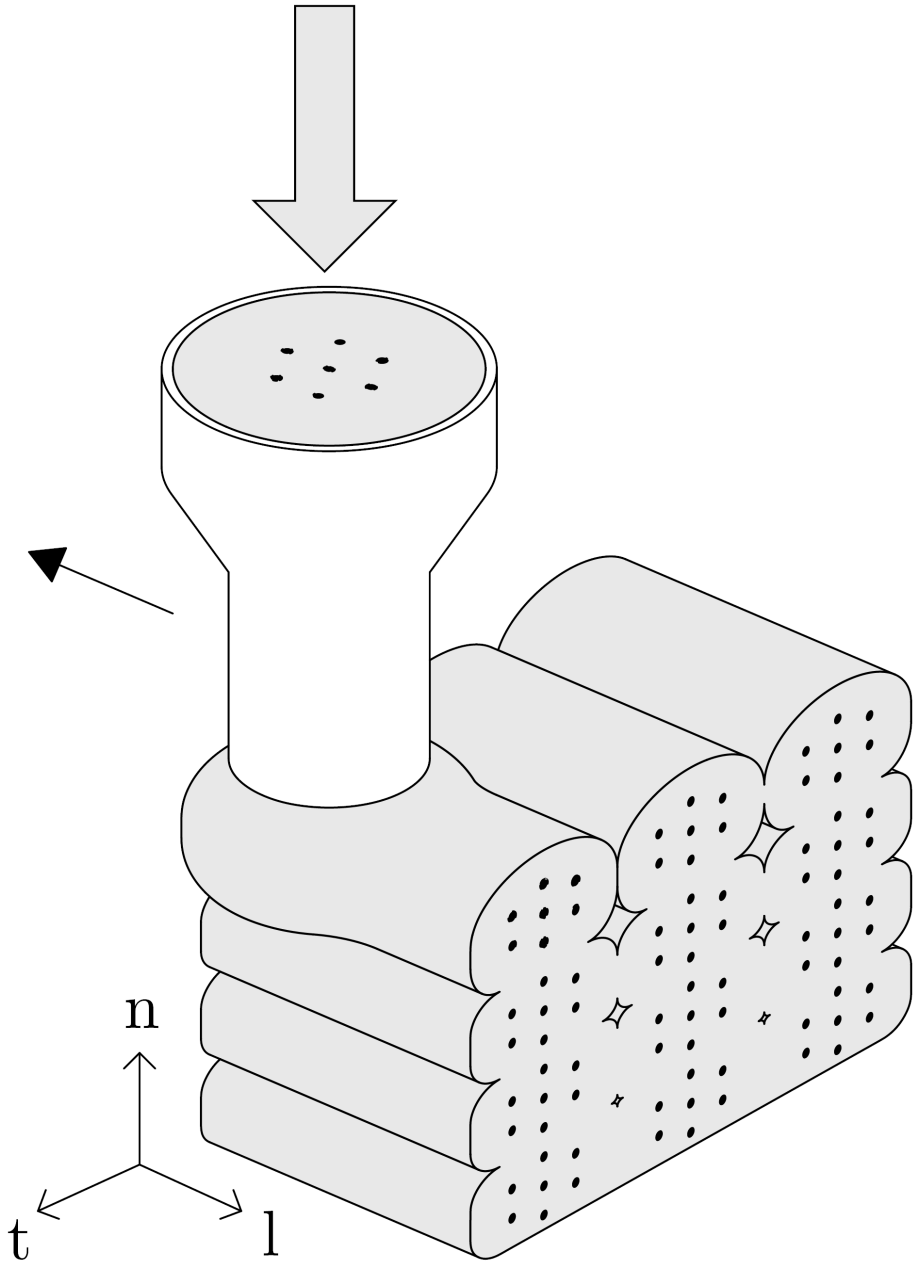

Figure 18: Schematic view of transverse isotropic arrangement of Flow-Based Pultruded laces. l is the printing direction

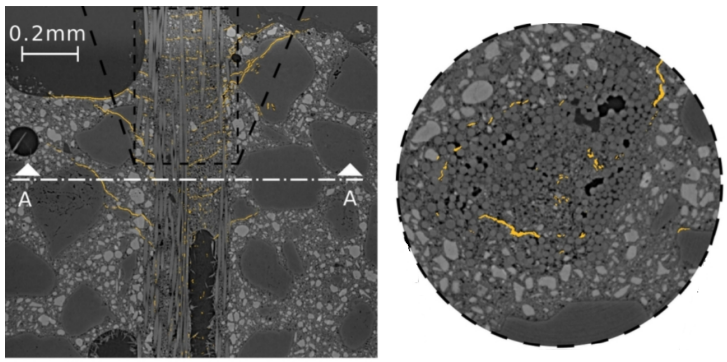

Figure 19: Transversal and longitudinal slices at the upper end of a speciment (basalt yarn/cement) at a force level of 34 N. micro cracks in yellow [19]

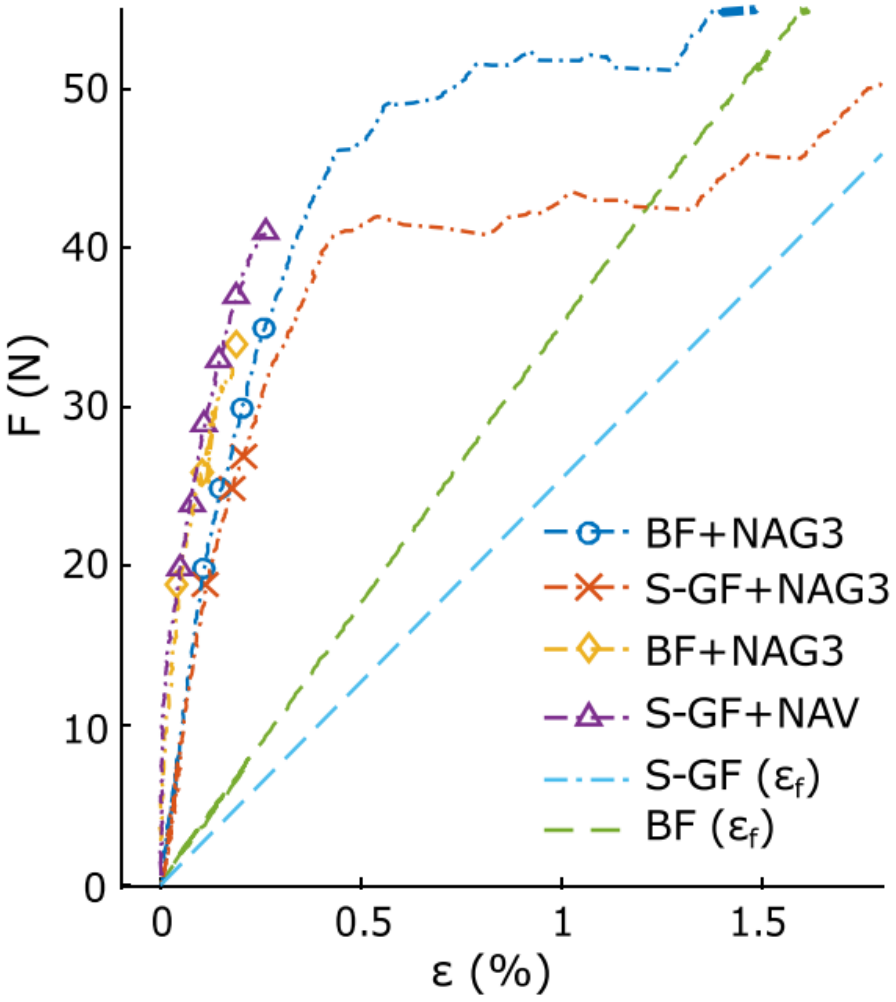

Figure 20: Tension stiffening force-elongation curves for different fibers/matrix combination and for yarns alone. BF and GF for Glass and Basalte Fibers (Punctual markers indicating the levels of loading for microtomographic investigations) [19].

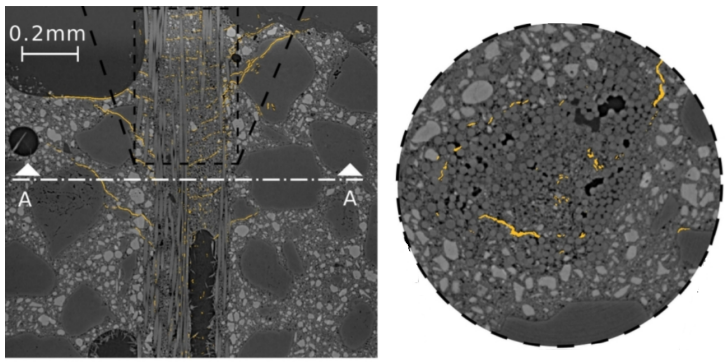

Figure 21: Transversal and longitudinal slices at the upper end of a speciment (basalt yarn/cement) at a force level of 34 N. micro cracks in yellow [19]

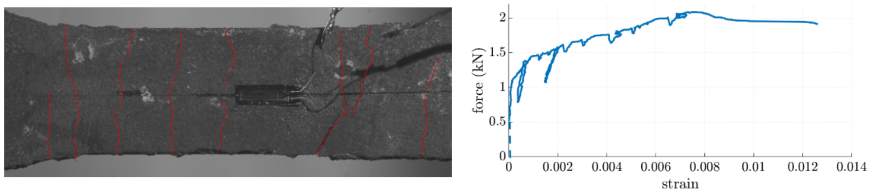

Figure 22: Direct tension test of anisotropic concrete specimen: Video capture of the test specimen at ultimate state showing multiple cracks highlighted in red, Force-strain graph depicting strain-hardening behaviour. Curve jumps are linked with cracking phenomena [18].

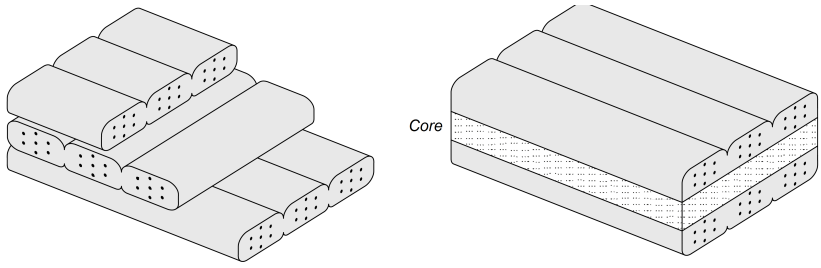

Figure 23: 2 directions printing for an orthotropic slab, and a sandwich architecture

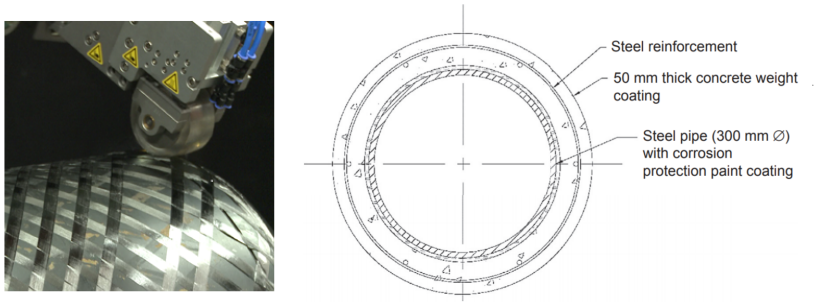

Figure 24: left:filament winding for CFRP (CETIM-France) - right Submarine steel pipe with concrete coating [44]